Electrical Transport Properties of IrO_2 and RuO_2†

W. D. RYDEN* AND A. W. LAWSON
University of California, Riverside, California 92507

AND

CARL C. SARTAIN‡
Technical Consulting and Manufacturing Company, Riverside, California 92507

(Received 30 April 1969)

The electrical resistivities of single crystals of RuO_2 and IrO_2 in the temperature range 10–1000°K are reported. It is found that electron-phonon and electron-electron interband scattering mechanisms account quantitatively for the observed temperature dependence of the resistivities. The Hall constants measured at 300 and 77°K are also reported.

I. INTRODUCTION

We report here the temperature dependence and magnitude of the resistivities and the Hall constants of the oxides RuO_2 and IrO_2. These oxides, together with several other oxides of the fourth and fifth transition series, exhibit metallic conductivities in the range 0.01–1 times the conductivities of the parent metals themselves. Several of these oxides have been reported by Rogers *et al.*[1] They include the oxides isoelectronic and isostructural to RuO_2 and IrO_2, which are OsO_2 and RhO_2,[2] respectively. Also the oxides, α-, β-ReO_2,[3] WO_2,[1] and MoO_2[4] have been found to be metallic. The cubic oxide ReO_3 is also metallic, with a conductivity which is slightly higher than that of metallic Re.[5]

IrO_2 and RuO_2 crystallize in the rutile structure, D_{4h}^{14}, with two molecules per unit cell. Their lattice parameters are identical within 2%, being $a=4.49$ Å, $c=3.11$ Å for RuO_2,[6] and $a=4.51$ Å and $c=3.15$ Å for IrO_2.[1] In this structure, the metal atoms, placed at the cell corner and body center, are very nearly octahedrally coordinated by oxygen atoms, with one axis of the octahedron being 4% shorter than the others. The electronic configuration for the cations, if the oxides are considered to be fully ionic, is $4d^4$ for Ru and $5d^5$ for Ir.

The determination of the intrinsic transport properties of oxides is often made difficult or impossible by surface properties or large defect concentrations which can dominate the transport properties or at least quickly mask intrinsic conduction mechanisms as the temperature is lowered. Work done on powdered oxides is notorious for being inconsistent with bulk properties. We found, for example, that sintered pellets of IrO_2 did not give the correct order of magnitude or the correct temperature dependence of the conductivity. Similar results are found by comparing the work of Gibart[3] on powdered ReO_2 with that of Rogers *et al.*[1] on crystals. Work on CrO_2 has also shown significant discrepancies between results obtained on powdered and single-crystal samples.[7]

Even when single-crystal oxides can be obtained, they often have defect concentrations which make them unsuitable for a study of their intrinsic properties. Fortunately, the dioxides of iridium and ruthenium can be obtained as single crystals which are relatively defect-free. We have been able to measure the resistivity of these oxides in the temperature range 4.2–1000°K, and we have been able quantitatively to account for their observed temperature dependence above 10°K. We find that a relation based on electron-electron and electron-phonon interband scattering gives a good fit to our resistivity data. The same relation has been used to account for the behavior of some of the transition metals.[8–10]

In Sec. II we describe the sample preparation and experimental apparatus. In Sec. III the experimental results are given. The fit to the temperature dependence of the resistivity and a discussion of the physical significance of the various parameters used in the fit is given in Sec. IV.

II. EXPERIMENTAL

A. Sample Preparation

In growing single crystals of these materials, we make use of the fact that both metals have volatile oxide species which decompose to form the dioxide. This vapor-transport technique of crystal growth for these two oxides has been described previously by Schäfer

† Work supported by the U. S. Atomic Energy Commission.
* Present address: Bell Telephone Laboratories, Inc., Murray Hill, N. J. 07974.
‡ Present address: Indiana State University, Terre Haute, Ind. 47809.
[1] D. B. Rogers, R. D. Shannon, A. W. Sleight, and J. L. Gillson, Inorg. Chem. **8**, 841 (1969).
[2] R. D. Shannon, Solid State Commun. **6**, 139 (1968).
[3] P. Gibart, Compt. Rend. **261**, 1525 (1965).
[4] A. Wold, W. Kunnmann, R. J. Arnott, and A. Ferretti, Inorg. Chem. **3**, 545 (1964).
[5] A. Ferretti, D. B. Rogers, and J. B. Goodenough, J. Phys. Chem. Solids **26**, 2007 (1965); J. Feinleib, W. J. Scouler, and A. Ferretti, Phys. Rev. **165**, 765 (1968).
[6] F. A. Cotton and J. R. Mague, Inorg. Chem. **5**, 317 (1966).
[7] D. S. Rodbell, J. M. Lommel, and R. C. DeVries, J. Phys. Soc. Japan **21**, 2430 (1966).
[8] A. H. Wilson, Proc. Roy. Soc. (London) **A167**, 580 (1938).
[9] W. G. Baber, Proc. Roy. Soc. (London) **A158**, 383 (1937).
[10] L. Colquitt, J. Appl. Phys. **36**, 2454 (1965).

et al.[11] Briefly, the technique involves flowing O_2 gas over the metal powder or metal oxide, the volatile species being transported in the gas stream down a temperature gradient until a point is reached where the volatile species decomposes forming the dioxide. Several crystal-growth habits were observed depending on the oxygen flow rate and temperature distribution. The orientations obtained in the case of IrO_2 were [001] and [011] needles and (011) and (100) plates. The orientations obtained in the case of RuO_2 were [001] needles and (011) plates.

The vapor-transport technique of crystal growth provides a large measure of crystal purification. The deposition of IrO_2 and RuO_2 crystals was found to occur at very particular sites in the apparatus according to flow rate and temperature. Thus, for impurities to occur in the grown single crystals, they must have an appreciable vapor pressure or volatile carrier and must condense under the same conditions of gas flow and temperature as the host crystal. Of course, impurities may also enter through the growth substrate. Using magnetic-susceptibility data we have inferred that ferromagnetic impurity concentrations are less than 10 ppm.[12] Spectroscopic analysis has shown the presence of 10 ppm Si and 15 ppm Al in both the RuO_2 and IrO_2 as well as 100 ppm of Ca in the IrO_2.[13] The residual-resistance ratio (RRR), $R_{(300)}/R_{(4.2)}$, may also be taken as a measure of sample perfection and was found to have values in the range 20–800. These ratios are not particularly high when compared with those obtained for pure metals. In view of the relatively high purity of our samples, the RRR which we obtain are probably attributable to lattice defects related to growth kinetics, rather than to foreign impurities, although we have not attempted a detailed study of this hypothesis.

The samples used for the transport measurements were taken as grown in most cases, although a few samples were cut to the desired orientation and shape by abrasion. The orientation of the crystals was determined by using a Laue back-reflection camera. The leads for the four-probe resistivity measurements and Hall-effect measurements were $\frac{1}{2}$- and 1-mil gold wires attached by thermal compression bonding. This involves heating the crystals to 400–500°C on the stage of a micromanipulator, placing the leads on the sample and crushing them with a 1×5-mil wedge using from 5×10^4–10^5 dyn of force. No strain could be detected in the region of the bond using Laue back-reflection photos. The sample dimensions were determined from photographic exposures at 500× and 75×, depending on sample size. In Fig. 1 an IrO_2 needle is shown on its alumina substrate along with an enlargement of one of its thermal compression bond leads. The gold lead wires from the sample were compression-bonded to platinum-gold islands on the Al_2O_3 substrates.

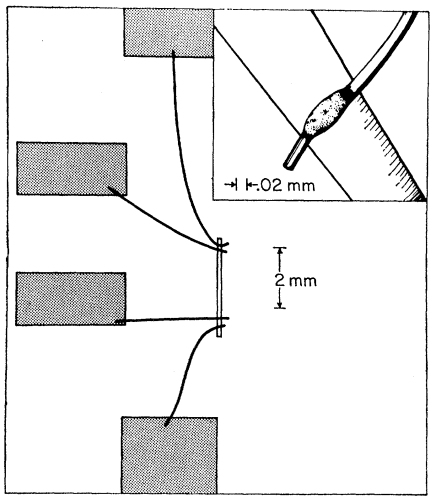

FIG. 1. IrO_2 *c*-axis needle is shown mounted with four electrical leads on an Al_2O_3 substrate. The inset shows an enlargement of a 1-mil gold wire bonded to the crystal.

B. Apparatus

The resistance measurements were made using a four-probe technique. Both dc and ac measurements were made. The dc potentials were measured by means of a Leeds and Northrup type K-3 potentiometer. The ac potentials were obtained using a Princeton Applied Research type HR8 lock-in amplifier. Heating effects were noted in some samples, and in such cases the ac apparatus was used. This latter apparatus has a voltage sensitivity which is three orders of magnitude higher than the dc apparatus, and it thus allows the current levels to be 2–3 orders of magnitude lower than those needed for the dc measurements. Care was taken to insure that stray capacitive and inductive pickup was negligible.

The resistance measurements in the temperature range from 4–300°K were obtained using both a cryostat and by direct immersion in liquid helium and liquid nitrogen. The cryostat is of standard design and is described elsewhere.[12] The temperature in this range was determined using a platinum resistance sensor (Rosemont Eng. Sensor H401) which was bonded along with the sample to an alumina chip by GE7031 varnish. Since the design of this sensor is somewhat nonstandard, it was calibrated against two other platinum resistors of more standard design.[14] These two calibrations agreed to within ±0.2°K over the range 10–300°K. The

[11] H. Schäfer and H. J. Heitland, Z. Anorg. Allgem. Chem. **304**, 249 (1960); H. Schäfer, G. Schneidereit, and W. Gerhardt, *ibid.* **319**, 327 (1963).

[12] W. D. Ryden, Ph.D. Thesis, University of California, Riverside, 1969 (unpublished); W. D. Ryden and A. W. Lawson (unpublished).

[13] B. Passenheim, Ph.D. Thesis, University of California, Riverside, 1969 (unpublished); B. Passenheim and D. C. McCollum, J. Chem. Phys. **51**, 320 (1969).

[14] We are indebted to B. Passenheim for the loan of these thermometers.

TABLE I. Resistivity of IrO_2 and RuO_2 determined at 300°K.

Crystal	Orientation	ρ_{300} ($\mu\Omega$ cm)
IrO_2:		
Ir6	[001]	51.0
Ir7	[001]	47.7
Ir22	[001]	48.5
		ρ_{av}[001]=49.1±0.5
Ir14	[011]	31.9; 36.3
Ir14′	[011]	34.0
Ir25	[011]	38.1
Ir26	[011]	34.2
		ρ_{av}[011]=34.9±1.0
RuO_2:		
Ru3	~[111]	35.5
Ru4	[111]	36.2
Ru5	[011]	32.8
Ru11	[011]	35.0
Ru10	[100]	36.1
Ru14	[001]	35.7
		ρ_{av}=35.2±0.5

uncertainty in temperatures determined using the Rosemont sensor was then taken as ±0.2°K.

The electrical resistance measurements in the temperature range 300–1000°K were made with the sample in a tube furnace. The temperature in the sample tube was determined from a Pt–(Pt-10% Rh) thermocouple. This thermocouple was periodically checked against a Pt–(Pt-13% Rh) thermocouple which had a calibration, accurate to within 1°K, traceable to the National Bureau of Standards. The crystals had electrical lead wires connected as in the low-temperature measurements. The lead wires out of the furnace were gold and they were compression-bonded to the platinum-gold terminations of the alumina substrate.

The Hall voltage was measured using a Honeywell six-dial potentiometer and a Leeds and Northrup electronic null detector. This apparatus allowed the Hall voltage to be determined to $\pm 5\times 10^{-9}$ V. We estimate that our Hall measurements are accurate to ±10% from the comparison of our results obtained for a polycrystalline copper sample and the previously reported Hall constants of copper.[15]

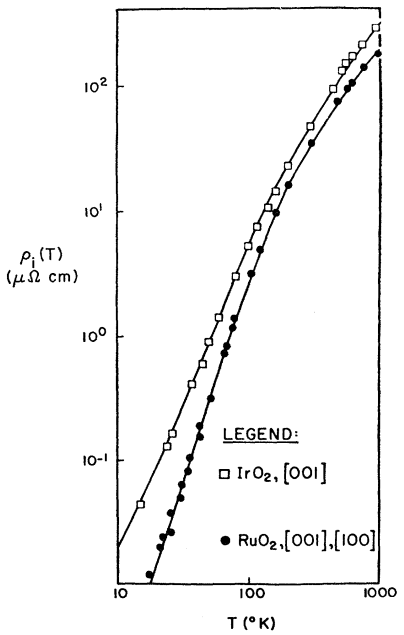

FIG. 2. Resistivity versus temperature of IrO_2 and RuO_2. The solid lines are obtained from Eq. (4).

III. RESULTS

A. Resistivity Magnitude

The resistivity tensor $\tilde{\rho}$ in the principal-axis system for a tetragonal crystal structure is determined by the principal resistivities, ρ_c and ρ_a. For the case of IrO_2, two different orientations were used to determine ρ_c and ρ_a, namely, [001] and [011]. Using the measured c-axis resistivity and the measured resistivity along [011], one finds

$$\rho_a=\frac{\rho[011]-\rho_c\sin^2\varphi}{\cos^2\varphi};\quad \tan\varphi=c/a. \tag{1}$$

Seven IrO_2 samples were used in the determination of $\tilde{\rho}$, three c-axis samples and four [011] samples. The resistivities for these samples are listed in Table I. The average resistivity values at 300°K are ρ_c=49.1 $\mu\Omega$ cm and ρ_a=27.8 $\mu\Omega$ cm.

The resistivity was determined for six RuO_2 samples (see Table I) in four different orientations. All of the samples gave the same resistivity value, 35 $\mu\Omega$ cm, at 300°K to within experimental error. The main contribution to the uncertainty in resistivity values comes from determination of sample dimensions which in some cases may be irregular to 10% of a particular dimension. The values of ρ_c at 295°K reported earlier by Schäfer *et al.*[11] are 48 $\mu\Omega$ cm and 50 $\mu\Omega$ cm for IrO_2 and RuO_2, respectively.

B. Resistivity Temperature Dependence

In this section the temperature dependence of the resistivities of single crystals of RuO_2 and IrO_2 are reported. The resistivities were obtained from resistance measurements in the range 4.2 to 1000°K. We have obtained the intrinsic resistance ratios from the relation

$$R_i=\frac{R(T)-R(4.2)}{R(300)-R(4.2)}, \tag{2}$$

where $R(T)$ is the total resistance at temperature T. The values of R_i were scaled by the resistivity values given in Table I to obtain the temperature-dependent resistivities. The results are shown in Figs. 2–4. The

[15] J. P. Jan, in *Solid State Physics*, edited by F. Seitz and D. Turnbull (Academic Press Inc., New York, 1957), Vol. 5, p. 45.

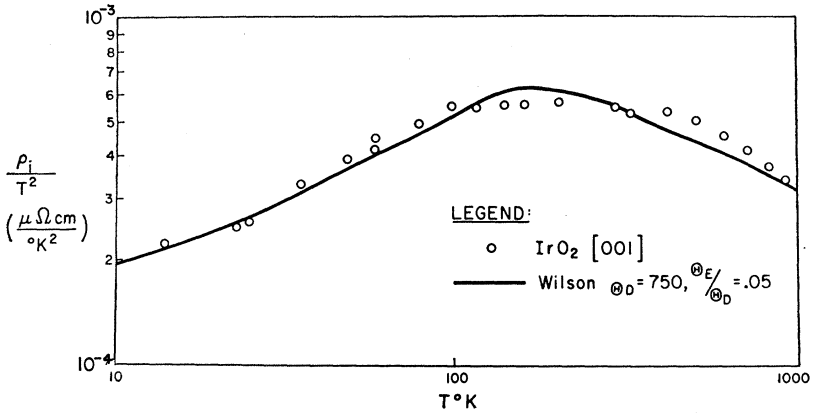

FIG. 3. Reduced resistivity ρ_i/T^2 plotted as a function of T for a c-axis IrO_2 crystal.

solid lines of these figures are a theoretical fit discussed below in Sec. IV.

The open squares of Fig. 2 were obtained from one c-axis IrO_2 needle. The same data divided by T^2 are shown in Fig. 3. Resistance ratios R_i were determined for a total of four IrO_2 crystals. Three of these were oriented along a [001] direction and the other was oriented along a [011] direction. The resistance ratios R_i of all of these samples showed the same temperature dependence to within experimental error down to 10°K. The residual resistance ratios, $R(300)/R(4.2)$, are in the range 20–50 for all of these samples except one [001] needle. This latter sample had an RRR of 500.

The solid circles of Fig. 2 are data from three RuO_2 samples. Two of these samples were oriented with the current along [111] and the third sample was oriented with the current along [110]. In Fig. 4, the quantity $\rho_i(T)/T^2$ is plotted versus T for sample Ru10. The resistance ratios R_i of six RuO_2 crystals were measured. These crystals were oriented along the [111], [011], [100], and [001] directions. The uncertainty in the data plotted in Figs. 3 and 4 has been determined from the instrumental uncertainty in determining R_i in Eq. (2) and from the temperature uncertainty. The uncertainty for the IrO_2 data shown in Fig. 3 ranges from $\pm 10\%$ at 10°K to $\pm 3\%$ at 25°K. For the RuO_2 data shown in Fig. 4, this uncertainty is $\pm 20\%$ at 9°K, $\pm 10\%$ at 13°K, $\pm 5\%$ at 16°K, and above 20°K it is negligible.

TABLE II. Hall constants and Hall mobilities of IrO_2 and RuO_2 determined at 300 and 77°K.

	Orientation H	Orientation J	$R(10^4$ cm³/A sec) 300°K	$R(10^4$ cm³/A sec) 77°K	μ(cm²/V sec) 300°K	μ(cm²/V sec) 77°K
RuO_2	$\perp(0\bar{1}1)$	[011]	−1.1	−0.79	3.1	61
	$\perp(0\bar{1}1)$	[100]	−1.2	−0.90	3.4	67
	$\perp(0\bar{1}1)$	[111]	−1.0	−0.75	2.8	55
IrO_2	[100]	[001]	+3.58	+4.70	7.3	120
	$\perp(0\bar{1}1)$	[011]	−2.60	−3.12	7.5	130

C. Hall Effect

The Hall constants at 300 and 77°K have been determined for two IrO_2 crystals and three RuO_2 crystals. The values are listed in Table II. The values for RuO_2 are isotropic to within $\pm 10\%$ and their sign indicates that electrons have the predominant mobility. The Hall constants of IrO_2 crystals show both electronlike and holelike behavior. For current directed along the c axis the Hall constant is positive and for current along [011] the Hall constant is negative. The Hall mobilities, taken simply as $\mu_H = R_H/\rho$, are listed in Table II.

IV. DISCUSSION

One of the major objectives of this work is to determine the scattering mechanisms which give the dominant contribution to the resistivity of pure RuO_2 and IrO_2. In principle, the temperature dependence of the electrical resistivity can be used to determine the conduction-electron scattering mechanism(s) (CESM) occurring in a particular metal. In fact, such a program

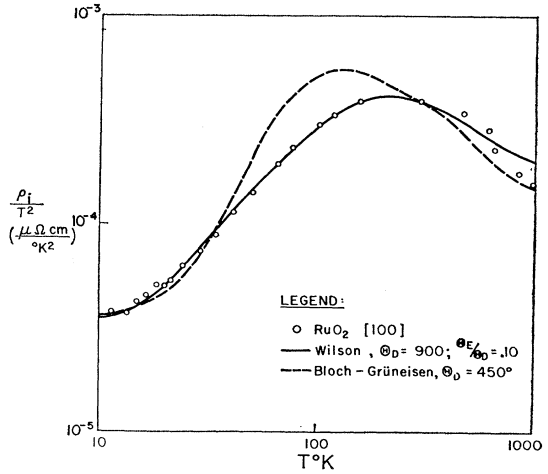

FIG. 4. Reduced resistivity ρ_i/T^2 plotted as a function of T for an a-axis RuO_2 crystal.

may give ambiguous results since it may occur that two or more CESM have nearly the same temperature dependence so that they cannot be distinguished in the available temperature range. It may also happen that there are deviations from Matthiessen's rule which give an additional temperature dependence apart from those of the intrinsic scattering mechanisms.[16,17] Although these difficulties have arisen in our analysis of $\rho_i(T)$ for these two oxides, we have been able to fit a relation based on two interband scattering mechanisms to the measured resistivities in the temperature range 10–1000°K.

In general, the resistivity of an isotropic metal can be written in the form

$$\rho(T)=\rho_0+\rho_i(T)+\Delta(T), \quad (3)$$

where ρ_0 is the total resistivity at $T=0$°K and is independent of temperature, $\rho_i(T)$ is the intrinsic resistivity of the defect-free metal, and $\Delta(T)$ is a temperature-dependent term arising from the nonadditivity of ρ_0 and $\rho_i(T)$.[16,17] The generalization of Eq. (3) to anisotropic metals could be quite complex. However, we find for these tetragonal crystals that the ratio $\rho_{ic}(T)/\rho_{ia}(T)$ is independent of temperature. It is then possible to make a single fit, except for a temperature-independent factor, to the two components of $\tilde{\rho}_i$.

The temperature dependence of ρ_i expected for various scattering mechanisms has been reviewed by Ziman[18] and by Wilson.[8] The roughly T^2 and T^3 temperature dependences of the resistivities which we have found for IrO_2 and RuO_2 are typical of some of the transition metals.[19] In particular, the T^2 and T^3 dependences of the resistivity of Pt and Pd below 30°K were shown originally by Baber[9] and Wilson[8] to be accounted for by electron-electron and electron-phonon interband scattering, respectively. These treatments followed Mott's proposal that the higher density of states and effective masses of the d-band holes would allow this band to act as a "trap" for the more mobile s-band conduction electrons.[20] These early treatments of interband scattering do not rely on the s or d character of the bands, but rather on the condition that there be an appreciable difference in the effective masses of these bands. It is not obvious that such a condition can be met in these oxides. It is usually assumed that the d bands contribute only low mobility carriers to conduction processes. However, in these compounds, high-mobility carriers may arise from the d-band manifold itself if appreciable hybridization with the oxygen p bands occurs. Although detailed energy-band calculations are not as yet available for RuO_2 and IrO_2, the recent calculation by Mattheiss[21] for ReO_3 illustrates the extent of p-d hybridization for this latter oxide. He finds that the width of the t_{2g} d manifold, ~4 eV, arises almost entirely from p-d hybridization. In general, this hybridization may vary considerably over the Brillouin zone depending on the details of the symmetry of the bands within the p and d manifolds. Thus it is reasonable to expect the Fermi surface to consist of several sheets having widely varying effective masses. In view of the observed temperature dependence of the resistivity of these oxides and the possible nature of the d bands as given above it is reasonable to try to account for the observed resistivity via the scattering mechanisms discussed by Baber[9] and by Wilson.[8]

The treatments of Baber[9] and Wilson,[8] when taken together, require ρ_i to be given by a relation of the form

$$\rho_i(T)=\rho_2T^2+\rho_3T^3[J_3(\Theta_D/T)-J_3(\Theta_E/T)], \quad (4)$$

where T is the absolute temperature, Θ_D is the usual Debye temperature, and Θ_E is a parameter characterizing the momentum gap between heavy- and light-mass bands. The function J_3 is a standard transport integral and has been tabulated.[10] The magnitude of the T^2 term is ρ_2 and the parameter ρ_3 is used to normalize Eq. (4) to the measured resistivity at 300°K. The contribution to the electrical resistivity from electron-electron interband scattering has been discussed more recently by Ziman,[18] Appel,[22] and Rice.[23] The second term on the right of Eq. (4), derived by Wilson, has been discussed recently by Colquitt[10] for the case of the transition metals.

The solid lines of Fig. 2 represent Eq. (4). The choice of the parameters in fitting the data to Eq. (4) is facilitated by the fact that each of the parameters ρ_2, Θ_D, and Θ_E dominate the temperature dependence over a particular temperature range. Thus ρ_2 is chosen to fit the resistivity in the range 10–20°K, where the electron-phonon term is small, and Θ_D is chosen to fit the resistivity in the temperature range above 100°K, where the fit is independent of ρ_2 and Θ_E. In the intermediate temperature range the parameter Θ_E can be chosen independently of Θ_D since in that range the function $J_3(\Theta_D/T)$ has a strictly T^3 dependence for a wide choice of Θ_D. This procedure requires that $\Theta_D/T \gtrsim 10$ in the intermediate temperature range.

The parameters required to fit Eq. (4) to the measured values of $\rho_i(T)$ are significantly different for the two oxides. The most striking difference between the parameters for the two oxides is the magnitude of the electron-electron term, it being ten times larger in the case of IrO_2. The uncertainty in the choice of electron-phonon parameters is larger in the case of IrO_2 than for RuO_2. The parameters and their uncertainty are indicated in Table III. The fit can be more clearly displayed

[16] M. Köhler, Z. Physik **126**, 495 (1949).
[17] E. H. Sondheimer and A. H. Wilson, Proc. Roy. Soc. (London) **A190**, 435 (1947).
[18] J. M. Ziman, *Electrons and Phonons* (Oxford University Press, London, 1963).
[19] G. K. White and S. B. Woods, Phil. Trans. Roy. Soc. London **251**, 273 (1959).
[20] N. F. Mott, Proc. Phys. Soc. (London) **47**, 571 (1935).
[21] L. F. Mattheiss, Phys. Rev. **181**, 987 (1969).
[22] J. Appel, Phil. Mag. **8**, 1071 (1963).
[23] M. J. Rice, Phys. Rev. Letters **20**, 1439 (1968).

TABLE III. Parameters of Eq. (4) as determined from the measured resistivities of IrO_2 and RuO_2.

	ρ_2 (10^{-5} $\mu\Omega$ cm/°K^2)	ρ_3 (10^{-7} $\mu\Omega$ cm/°K^3)	Θ_D(°K)	Θ_E/Θ_D
RuO_2	3.5±0.5	3.2	900±50	0.1±0.02
IrO_2	17.7±0.8	5.56	700±100	~0.05

by dividing out the T^2 dependence in Eq. (4). A plot of ρ_i/T^2 versus T is shown in Figs. 3 and 4 for IrO_2 and RuO_2, respectively.

Several alternatives to Eq. (4) were tried. However, no improvements in the fit listed in Table III could be obtained. The best fit which uses a strictly Bloch-Gruneisen formula also is shown in Fig. 4.

In fitting ρ_i in Eq. (4) to the measured resistance ratios given by Eq. (3), we have assumed that Matthiessen's rule is valid. This assumption is justified if it is found that R_i in Eq. (2) is the same for samples having different RRR. In the case of IrO_2 this condition was found to be valid for our crystals, which had RRR in the range 20–500. In the case of RuO_2 it was difficult to establish the dependence of R_i on RRR since most of the samples had the same RRR. One RuO_2 sample which appeared "erroded" had a RRR which was 10× less than the other RuO_2 samples and deviations from Matthiessen's rule were found. Although the behavior of this sample may not be typical of lower RRR samples, we have used it to estimate an upper limit on the possible deviations from Matthiessen's rule for RuO_2. These upper limits are found to be 30% at 20°K, 15% at 30°K, 7% at 40°K, and 3% at 60°K. These uncertainties do not affect the choice of Θ_D, but they are the major source of uncertainty in Θ_E and ρ_2.

For these oxides the magnitude of the T^2 term, ρ_2, of Eq. (4) which we find is comparable to those of some of the transition metals. A few of these values are as follows: (in units of 10^{-5} $\mu\Omega$ cm/°K^2) Pd, 3.3; Pt, 14; Mn, 15 000;[19]; and IrO_2, 18; RuO_2, 3.5. The physical significance of the magnitude of the T^2 term in Eq. (4) is not clear since several scattering mechanisms have a T^2 temperature dependence. Besides the scattering of electrons by a screened Coulomb interaction, discussed by Baber, the scattering of s-band conduction electrons by fluctuations in the uniform spin density of the d band via an exchange interaction also gives a T^2 temperature dependence. This latter mechanism has been the subject of more recent work treating the low-temperature resistivity of Pd and Pd-Ni alloys.[24] In any case, independent determinations of the parameters of the Fermi surface such as the Fermi energy and the band effective masses as well as screening lengths would be required before detailed comparisons between theoretical expressions and measured values of ρ_2 could be made. This information is, for the most part, unknown.

The temperature dependence of the resistivity given by the Wilson term in Eq. (4) can be summarized as follows. At high temperature the resistivity is a linear function of temperature. At temperature below $\Theta_D/5$ the resistivity varies as T^3 and as the temperature is lowered still further the resistivity varies ultimately as $e^{-\Theta_E/T}$ for $T<\Theta_E/5$. The T and T^3 dependence has often been observed.[21] However, the ultimate exponential dependence has never been unambiguously observed.

The difficulty in observing this latter behavior lies in the fact that the type of metal which exhibits electron-phonon interband scattering also exhibits electron-electron scattering. The magnitude of the resistivity attributed to the latter scattering mechanism dominates the total resistivity in the temperature range where the exponential dependence should appear. Considering typical residual resistivities, we find that it is then necessary to resolve the total resistance to parts in 10^3–10^5 in order to see the phonon resistivity.

Up to this point in our discussion, we have neglected the possibility that the interband contribution to the resistivity becomes equal to the intraband contribution. If this occurs at temperatures above the exponential region of the Wilson formula, then this latter region will in principle be unobservable. In any case, the parameter Θ_E can be evaluated in a temperature range above that required to see the exponential behavior since the resistivity decreases significantly faster than T^3 in the range $T<\Theta_E$. In the case of Pt and Pd, the values of Θ_E obtained from resistivity measurements are in good agreement with those estimated from the empirically determined Fermi surface.[25] Although the parameter Θ_E can, in principle, be calculated using the sound velocity and Fermi-surface dimensions,[25] neither the sound velocities nor enough detailed information about the Fermi surfaces of these oxides is known to allow such an estimate to be made.

In the case of RuO_2 it is interesting to see to what extent the electron-phonon resistivity approaches the exponential region predicted by Wilson. In Fig. 5 we plot the Wilson term in Eq. (4) versus Θ_E/T in the temperature range $T<\Theta_E$. For $\Theta_E=90$°K, the Wilson term in Eq. (4) becomes strictly exponential (the dashed line of Fig. 5) below 10°K. The open circles of Fig. 5 are the data points for sample Ru10 with the term ρ_2T^2 in Eq. (4) subtracted. In plotting these data, no account has been taken of the possible deviations from Matthiessen's rule discussed above. For this reason, the conclusion that the exponential region may be observable in RuO_2 is unreliable. Further measurements on higher RRR samples in the region extending below 10°K are required.

The values of the Debye temperature we obtain for IrO_2 and RuO_2 by fitting the Wilson term in Eq. (4) in the region 100–300°K are some 50% higher than the values obtained by Passenheim from specific-heat

[24] A. I. Schindler and M. J. Rice, Phys. Rev. **164**, 759 (1967).

[25] W. D. Ryden, Solid State Commun. 6, 847 (1968).

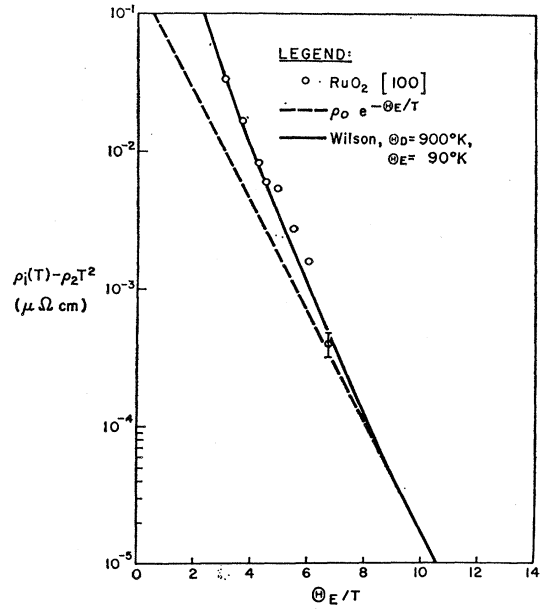

FIG. 5. Wilson term in Eq. (4) is plotted versus Θ_E/T showing the exponential behavior expected for this term at the lowest temperatures.

measurements. For the purposes of this discussion we label the resistivity Debye temperatures Θ_R, and the specific-heat Debye temperatures Θ_D. The values of Θ_D for RuO_2 and IrO_2 were obtained from the coefficient of the T^3 term of the specific heat in the region 0.5–10°K.[13] In general, for the monovalent metals, the agreement between Θ_R and Θ_D is much better than that reported here for RuO_2 and IrO_2. Blackman[26] has pointed out that the agreement between Θ_R and Θ_D for many metals is fortuitous considering the assumed lattice models. He argues that, since the formulation of the resistivity assumes only the presence of longitudinal lattice vibrations while the specific heat includes both longitudinal and transverse vibrational modes, the two parameters should differ. He calculates the Debye temperature for Al and W from the average longitudinal sound velocity and compares it with a similar calculation including both longitudinal and transverse modes. He finds for aluminum, $\Theta_L=707$°K and $\Theta_D=415$°K, and for tungsten, $\Theta_L=636$°K and $\Theta_D=384$°K. These calculated differences between Θ_L and Θ_D are similar to those between Θ_R and Θ_D determined for RuO_2 and IrO_2. This suggests that only longitudinal lattice vibrations are effective in scattering electrons for these two oxides. In the case of the monovalent metals, particularly the noble metals, it has been argued by Ziman[18] that both longitudinal and shear waves scatter electrons equally and would thus account for the agreement of Θ_R and Θ_D in those metals. Although the above argument for these oxides may be correct, it requires that shear waves be ineffective in scattering electrons in these oxides, and this supposition is not obvious.

It is found that both Θ_R and Θ_D for RuO_2 and IrO_2 nearly scale as

$$\frac{\Theta_D(RuO_2)}{\Theta_D(IrO_2)}=\left[\frac{M(IrO_2)}{M(RuO_2)}\right]^{1/2}=1.3, \qquad (5)$$

where M is the molecular weight of the dioxide molecule. We find from resistivity measurements $\Theta_R(RuO_2)/\Theta_R(IrO_2)=1.3$, and Passenheim and McCollum[13] find from specific-heat measurements $\Theta_D(RuO_2)/\Theta_D(IrO_2)=1.35$. If the elastic constants of these two oxides are the same, then a relation of the form of Eq. (5) follows from a Debye model of a solid composed of dioxide molecules. This relation should hold regardless of the contribution of the longitudinal and transverse phonons to Θ_R and Θ_D.

The interband nature of the scattering mechanisms discussed here implies that the Fermi surfaces of these oxides consists of several sheets of quite different effective-mass carriers. In the case of RuO_2 this has to some extent been confirmed. Both the de Haas–van Alphen measurements of Marcus and Butler[27] and the magnetothermal oscillation measurements of Graebner and Ryden[28] have confirmed a Fermi surface consisting of at least two sheets of appreciably different mass carriers.

[26] M. Blackman, Proc. Phys. Soc. (London) A64, 681 (1951).

[27] S. M. Marcus and S. R. Butler, Phys. Letters 26A, 518 (1968).

[28] J. E. Graebner and W. D. Ryden (unpublished).